A Stochastic Simulation of the Failure Process and Ultimate Strength of Blended Continuous Yarns

MARY LYNN REALFF

School of Textile and Fiber Engineering, Georgia Institute of Technology, Atlanta, Georgia 30332, U.S.A.

NING PAN,[1] MOON SEO,[2] MARY C. BOYCE, AND STANLEY BACKER

Department of Mechanical Engineering, Massachusetts Institute of Technology, Cambridge, Massachusetts 02139, U.S.A.

ABSTRACT

The mechanics of the failure process and ultimate strength of a twisted yarn structure are studied using a newly proposed stochastic model of the failure process. The importance of the twist reinforcing mechanism to the strength of a twisted structure with continuous components, the interaction patterns between different component types during yarn extension, and the significance of multiple breaks along a component are demonstrated. Building on the three basic concepts of fragmentation and chain-of-sub-bundles, changing lateral constraint between components due to twist and its effect on component strength, and load sharing between broken and still surviving members during yarn breakage, a new mechanistic approach is proposed and a stochastic computer model is developed to predict the behavior of blended yarns. The approach is similar to that developed earlier by Boyce *et al.* [3] to study the failure process in woven fabrics. The model acts to predict the strength and fracture behavior of a blended yarn with continuous components. The predicted results are illustrated in comparison with the experiments of Monego *et al.* [20, 21, 22]. By means of this new model, fundamental features of blended yarn behavior are simulated and elucidated, including the strength reinforcing mechanism of twist in a blended yarn, the yarn break propagation pattern, and the effect of twist on yarn fracture behavior as well as the shape effect of component stress-strain curves. Moreover, the relationship between the strength of a structure and that of its components is also investigated.

Fiber blending has traditionally been considered an effective means for improving or reinforcing mechanical as well as other properties of yarns. The study of blended continuous-filament structures has attracted the attention of many researchers [2, 15, 19, 20, 21, 22, 23]. The purpose of such study is to understand the role of various phenomena contributing to the mechanical behavior of the blend, including the reinforcing mechanism of fiber blending, the interactions of the different constituent fibers in a hybrid twisted structure under external load as well as the effect of lateral pressure on fiber interaction, the relation and mechanism between yarn strength and blend ratio, and the effect of twist level on the fracture behavior of blended yarn. Ultimately, results from these studies will provide theoretical foundations for predicting the ultimate strength and fracture behavior of blended filament yarns. This is significantly important to textile science, and could potentially help fiber producers and textile firms guide fiber processing and optimize textile blending and spinning techniques.

Many investigators have focused on filament yarns, not only because the filament structure has considerable significance for certain industrial applications, but because the study of continuous filament yarns is also mathematically more manageable compared with staple yarns, and will certainly provide a basis for further development of the theory for staple yarns.

Research on the strength and fracture behavior of blended filament yarns involves the investigation of frictional interactions of fibers (filaments), fiber flaw distribution and its effect on yarn strength, fiber *in situ* mechanical properties, and stress transfer from a broken fiber into still surviving fibers during yarn extension. Some of these issues are also of interest to researchers in

[1] Present address: Division of Textiles & Clothing, and Biological and Agricultural Engineering Department, University of California, Davis, CA 95616.

[2] Present address: Kunkuk University, Seoul, Korea.

fiber composite materials, and some are fundamental to materials science in general.

To understand and predict the strength of filament yarns accurately, another major parameter has to be considered, that is, the effect of transverse pressure on the individual fibers due to tensioning of the yarn. The importance of lateral pressure on load transfer from fiber to fiber in a twisted fibrous structure was recognized as far back as Galileo [6], and several researchers in yarn mechanics have incorporated the effect of the transverse force into their analytic models. For example, Gurney [9] developed a relationship between yarn strength, twist level, lateral contraction ratio, and fiber stress-strain properties. Sullivan [35] determined the strength of staple fiber yarns by analyzing the lateral pressure distribution across the yarn and its contribution to axial stress. Machida [19] analyzed the lateral pressure in blended filament yarns under tension as a means of predicting the recovery fiber length during yarn rupture. Grosberg *et al.* [8] calculated lateral pressure distribution in a low-twist sliver under extension so as to predict sliver strength. Dogu [4] derived the distribution of transverse pressure in a twisted yarn, including fiber migration and fiber packing density variation. Hearle *et al.* [11], Kilbey [16], and White *et al.* [37] provided a comprehensive analysis of filament yarn strength, taking into account transverse forces and leading to a more complete understanding of the relationship between filament and yarn properties.

Meanwhile, in view of the stochastic nature of material strength, statistical approaches have been applied as well. Phoenix [25, 26, 27] proposed the concept of the chain-of-bundles model of yarn strength to tackle the issue of the statistical nature of strengths of individual filaments and yarns, the size (length) effect on filament strength, and the load sharing mechanism during yarn breakage. Boyce *et al.* [3] extended this kind of chain-of-bundles model to include interactions of model elements (yarns) to predict failure in woven fabrics.

Despite all these studies, a number of questions about filament yarn strength and fracture behavior remain unanswered. The salience of these problems, as summarized below, is often revealed in industrial practice.

According to existing analyses, the initial singles yarn rupture should always take place at the center where the filament strain is the greatest. While this occurs in certain yarns, it is by no means universal, as shown in experimental work [19, 21].

Most earlier models assumed that once a filament in a yarn breaks, it ceases to contribute to yarn strength. However, the presence of multiple breaks along a single filament in a tensioned yarn observed experimentally [19, 21] and termed the "fragmentation phenomenon" in the composites area, illustrates the invalidity of such an assumption and suggests that a broken filament is still subjected to the full level of yarn strain at positions removed from the broken end, due to interfiber friction acting to transmit load.

The strength of materials is already proven to be statistically related to material dimensions as well as the structures in which they function [18, 24, 32, 34]. In the case of tensioned yarns, the effective length on which the strength of a filament should be determined is proven to be different from its original length, as illustrated in the next section. Moreover, the filament itself is under a complex stress state when tensioned, and a changing lateral pressure is exerted on it. These factors inevitably alter the apparent strength of the filament and suggest the invalidity of using filament properties tested in conventional conditions, isolated from the yarn, to build a theoretical model.

Furthermore, researchers [27] in the area of fiber and yarn mechanics have long been intrigued by the fact that stronger fibers do not necessarily lead to a stronger yarn. They have suggested some models that try to explain the cause of this lack of correlation between fiber and yarn strength.

Therefore a more realistic blended filament yarn model is desirable, and as an attempt in this direction, we have developed an alternative model in this paper. The model addresses the prediction of load-extension behavior, strength, and fracture behavior in blended filament yarns, as well as ropes and other similar twisted flexible structures, based on fiber properties, blend ratio, yarn structural parameters, and yarn twist level.

Experimental Evidence

To illustrate our model clearly, we present an early study on this issue in detail here. The importance of this prior work is that it delivers informative and elaborate experimental evidence obtained under conditions close to ideal, and hence reveals a few fundamental points that have not yet been incorporated in the existing yarn analysis. Also, unprecedentedly the whole experimental work is so thorough that it provides a very valuable base to verify theoretical predictions.

In an experimental investigation, Monego *et al.* [20, 21, 22] studied the rupture mechanisms in continuous twisted structures of blended fiber types using mechanical tracer elements. To facilitate experimental control and observation, they made a set of gross-model yarns in lieu of conventional structures. The gross-model yarns each consisted of 91 components, either cotton yarns or polyester (termed PET or Dacron below) filament yarns, drawn from independent packages in a creel and twisted carefully with negligible radial migration in five helical layers about a central or core yarn. In all, 91 different colors were used for different samples of the cotton yarn

to permit identification of each cotton component with respect to its radial position in the gross model. They prepared a range of such model structures that varied from 0% to 100% cotton (100% to 0% polyester) with twist ranging from about 0.50 to 4.50 twist multiplier.

In these model yarns (or more accurately, strands consisting of individual yarns or components), the polyester components were yarns of 70 denier formed by 34 filaments. The cotton yarns were 67 denier. For brevity, however, in our study we will refer to the model strand as a blended yarn and its constituent yarns as components.

Successive specimens of these model strands were tension tested to different strain levels. After each specimen was strained to its designated level, it was removed from the instrument, then carefully untwisted and examined for the presence of tensile breaks in the component yarns. A fairly simple approach was used to record the location and frequency of component breaks at each extension level for each gross-model. A series of parallel lines drawn in groups corresponded to one-half the number of components in each ring of the model cross section. Each group was then arranged symmetrically about the center line or axis of the model. The lines were numbered arbitrarily from right to left, as shown in Figure 1. Thus, each numbered line corresponded to a numbered position in the cross section of the model in Figure 2. The unmarked locations represent polyester yarn positions for the given specimen. A few testing results are provided here as a basis for further discussion.

Figure 2 shows data taken in tests of a 2-cotton/89-polyester component model, with the cotton located at positions 8 and 52 as shown, and a twist multiplier of 2.19. After extension of the model yarn to the 11% strain level, component 52, located in the second ring from the core, evidenced five breaks in its 20.32 cm gauge length, while component 8 in the fifth or outer ring showed no breaks, as seen in Figure 1a. When another specimen of the same model was extended to 15%, it evidenced 19 breaks in component 52 and fewer breaks in 8, as shown in Figure 1b. Figure 1c, representing the effect of 25% extension, shows the presence of 44 breaks in component 52 and 13 in component 8.

As mechanical tracers, components 52 and 8 clearly illustrate the dependence of multiple break frequency on location, hence on local strain level and on local pressure. Similar conclusions can be derived from Figures 3 and 4, showing a 4.37 twist multiplier model with 10 cotton and 81 polyester components.

In contrast, an entirely different fracture behavior can be observed by using a 3.26 twist multiplier model of 39 cotton components. Rupture initiation of a few inner cotton components is followed by rapid and concentrated propagation of the break to most of the cotton yarns in that region. At this point, the load shed so precipitously by the cotton exceeds the additional load bearing capacity of the polyester, and the entire model fails in a manner characteristic of a 100% cotton model. The remaining elongation of the polyester is not realized, as shown in Figure 5. The concentration of the break propagation is seen in Figures 6a, b and c for extension steps of 11%, 12%, and 13%, respectively.

Finally, Figure 7 shows that twist strongly influences load transfer and rupture propagation. Here, all yarns have the same blend ratio of 56% cotton/44% polyester, and the twist levels vary from 0.54 to 4.34 twist multiple. Twist is observed to affect component independence, yarn tensile strength, achievement of (or failure to reach)

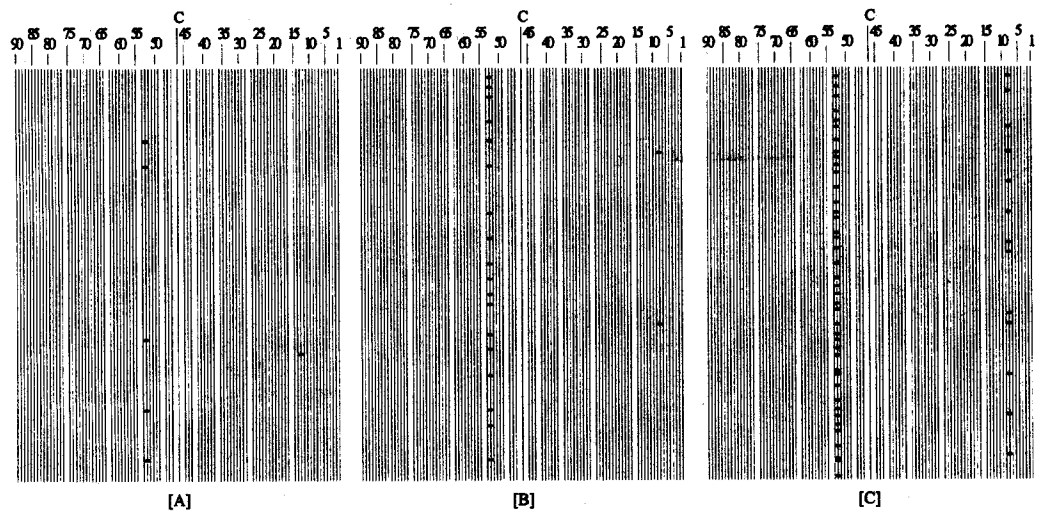

FIGURE 1. Experiments of a model yarn with 2 cotton and 89 Dacron components at $TM = 2.19$ [20]: (a) multiple breaks at 11% extension, (b) multiple breaks at 15% extension, (c) multiple breaks at 25% extension.

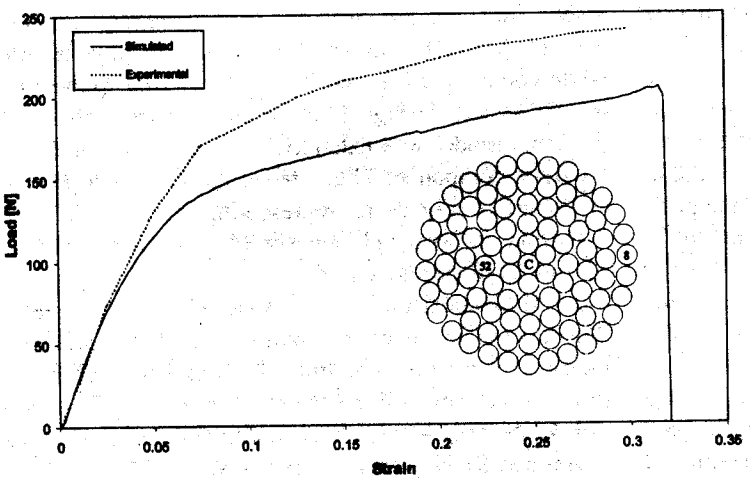

FIGURE 2. Yarn cross section with experimental [20] and simulated response of a model yarn with 2 cotton and 89 Dacron components at $TM = 2.19$.

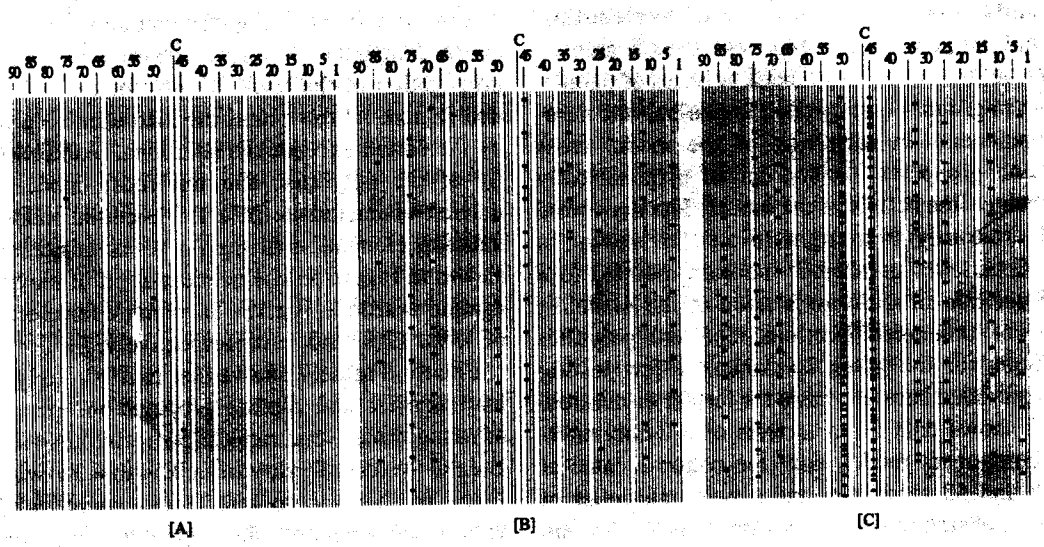

FIGURE 3. Experiments of a model yarn with 11 cotton and 80 Dacron components at $TM = 4.37$ [20]: (a) multiple breaks at 11% extension, (b) multiple breaks at 14% extension, (c) multiple breaks at 30% extension.

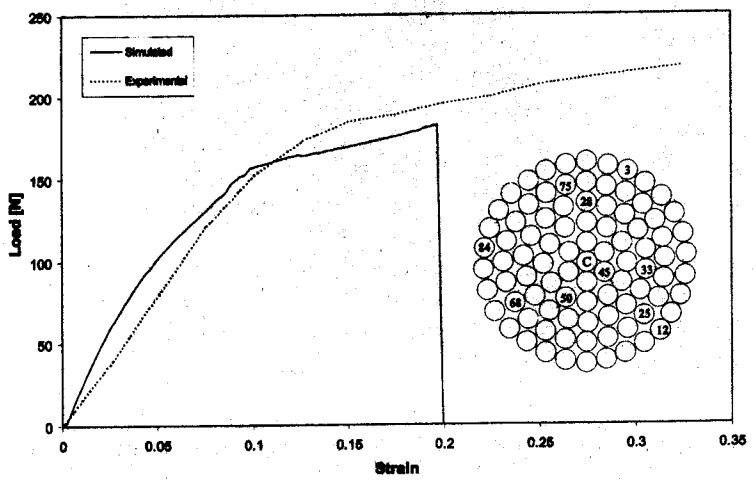

FIGURE 4. Yarn cross section with experimental [20] and simulated response of a model yarn with 11 cotton and 80 Dacron components at $TM = 4.37$.

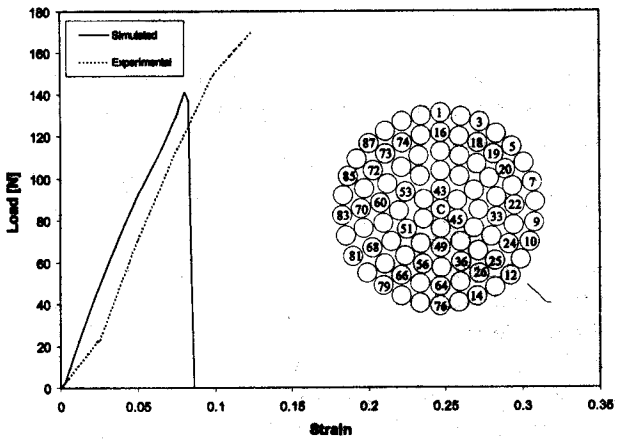

FIGURE 5. Yarn cross section with experimental [20] and simulated response of a model yarn with 40 cotton and 51 Dacron components at $TM = 3.26$.

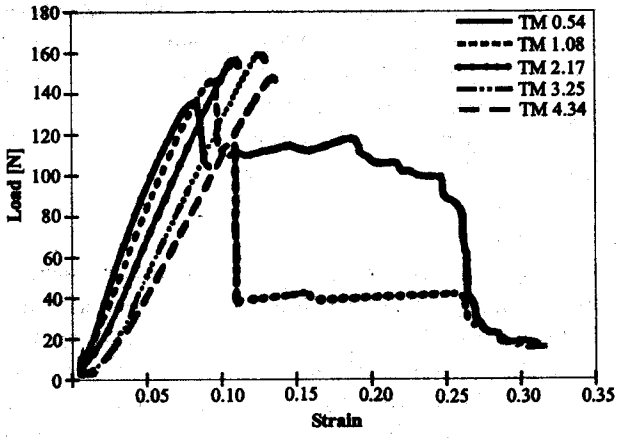

FIGURE 7. Effects of twist level on fracture behavior of model yarns (experimental [20]).

full filament extension, overall shape of the yarn stress strain curve and its general slope and, eventually, the work to tensile rupture.

Reinforcing Effect of Twist

To further demonstrate the reinforcing mechanism of twist to yarn structure and the contribution of lateral compression to yarn strength, some calculations and comparisons may be helpful. An example is taken from Figure 4, which shows a 4.37 twist multiplier yarn with 10 cotton and 81 polyester components. We will demonstrate the reinforcing effect of twist by comparing three different assumed structures made from these 91 components.

THE ACTUAL YARN

As shown in Figure 4, the experimentally determined breaking strength of this structure is $T_1 = 233.5$ N.

A Structure of Parallel Filament Bundles

The yarn is now idealized as a system consisting of 91 components parallel to each other without interaction. The average breaking strength of the components has been experimentally determined as 1.20 N (cotton) and 2.40 N (polyester). Now, assuming all components reach

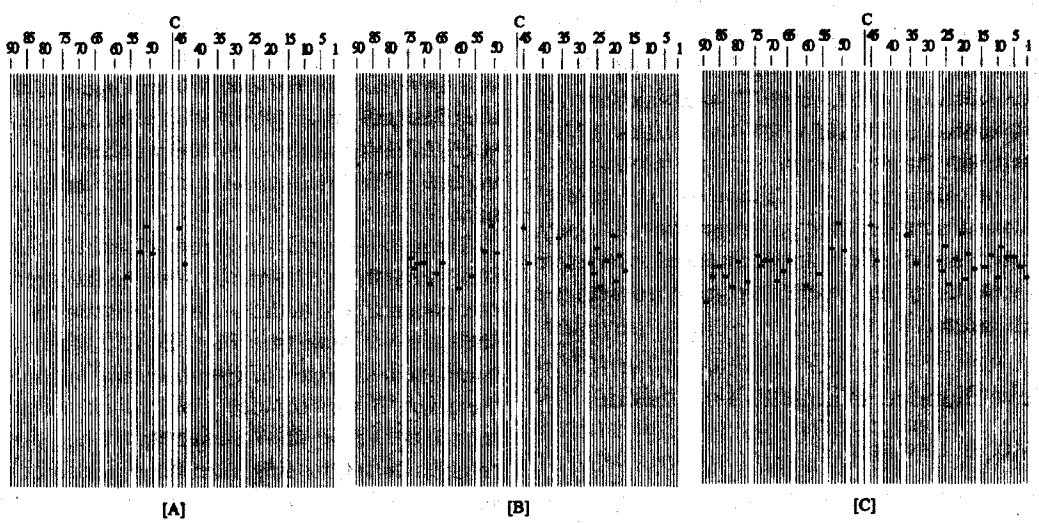

FIGURE 6. Experiments of a model yarn with 40 cotton and 51 Dacron components at $TM = 3.26$ [20]: (a) multiple breaks at 11% extension, (b) multiple breaks at 12% extension, (c) multiple breaks at 13% extension.

their full strength, then the highest possible strength of this whole structure will include the contribution of cotton components, T_c = 12.0 N, and the contribution of polyester components, T_p = 194.4 N. The strength of the entire structure is T_2 = 206.4 N.

A Twisted Structure Without Intercomponent Interactions

The structure is now idealized as a twisted structure without intercomponent interactions. In this case, the calculation takes into account the filament helix angles, which change during yarn tension. If the yarn volume is assumed to be constant during yarn extension, based on the 33% breaking elongation indicated in Figure 4 and using the relationships between yarn geometric parameters [11], the ultimate helix angle of the yarn under 33% elongation can be roughly expressed as

$$\tan q_{u,i} = \frac{\tan q_{o,n}(1 - \nu_y \epsilon_y)}{1 + \epsilon_y} = 0.7395 \times \tan q_{0,n} , \quad (1)$$

where ν_y = 0.5 and ϵ_y are the yarn lateral contraction and strain, and $q_{u,n}$ and $q_{0,n}$ are the ultimate and the original helix angles for each layer n of the yarn.

The maximum breaking strength of this structure can be calculated as [27]

$$T_3 = \sum_{n=0}^{5} [(N_{D,n}(2.40 \text{ N}) + N_{C,n}(1.20 \text{ N})) \cos q_{u,n}]$$

$$= 195.19 \text{ N} \quad . \quad (2)$$

Of these three strength values, the experimentally determined strength T_1 is the highest. This has to be attributed to the reinforcing effect of interfiber interference in a twisted structure since, without this interference, the maximum strength of a yarn as indicated by T_3 only reaches about 80% of its real strength. Note that 80% is still an overestimated value, since T_3 was calculated at the most favorable condition when we assume all the components fulfill their maximum strength. Considering the discount of component contribution to yarn strength in a real twisted structure due to component obliquity, the significance of the effect of twist-caused interaction between fibers due to the lateral compression within a yarn is even greater.

A New Blended Filament Yarn Model

General Model Description

From this experimental work, we can make many interesting observations and thus some assumptions to form the basis for the new theoretical model introduced in this paper.

First, as seen in Figures 1, 3, and 6, the presence of multiple breaks along a single cotton component illustrates the invalidity of the assumption that a broken filament in a yarn ceases to contribute to yarn strength. For even though the cotton component fails a few times, it is still subjected to the full level of the local strain at positions removed from the broken end. This buildup in local stress (or strain) from zero at the position of the break to the yarn strain at the given radius occurs through a frictional mechanism.

Multiple breaks on one filament, prior to failure of the total system, have been documented by researchers in the composite materials field [5, 33] and result from load transfer from the matrix by means of shear lag. The fact that one break at a position doesn't prevent other parts of the same component from being tensioned and successively broken again implies the independence of each filament segment from other segments of the same filament in terms of mechanical response to external load, although they are physically connected to each other. This phenomenon has been modeled for filament composite materials [12, 13, 14, 28]. When modeling filament yarns, the minimum length of each filament segment, the so-called "critical length" [3, 5, 33], is determined by the lateral pressure, the interfilament frictional property, and the filament breaking strength. Thus, it differs corresponding to different kinds of fibers and different radial locations within the yarn, and it also changes continuously during yarn extension. Therefore, in a twisted structure, mechanically each filament can be treated as a chain of independent filament segments of changing number and length. Furthermore the breaking strength of each segment on the same filament may vary because of the statistical nature of material flaw distribution over a filament length.

The results of Figures 1, 3, and 6 show that multiple breaks occur along a filament; however, yarn strength is still governed by the transverse propagation of component filament breakage. In other words, as expected, yarn strength is determined by the weakest link of the yarn instead of the weakest link of each individual component.

These observations suggest a statistical treatment of yarn strength by statistically treating the strength of each component. To address the statistics of component strength, we note (see Figures 1, 3, and 6) that each component changes in length during tensioning due to breakage. If we consider a component to be a chain of segments where the number and length of segments changes during loading, then the dependence of segment strength on length must be taken into account. It has long been recognized that a material's strength is statistically related to its dimensions, as governed by the well-known weakest-link theory [24] and shown for yarns by Realff

et al. [32]. According to the theory, the tensile strength of a specimen increases with its decreasing length. Therefore, the effect of changing length of these segments during yarn extension has to be considered when predicting yarn strength. Note that the increase in filament load will increase the slip length or exclusion zone in the presence of constant lateral pressure [27]. However, the observed decrease in filament segment length with loading indicates that the increase in lateral pressure is the dominant effect on critical length.

Also, the experimental results [21] provided in Figure 7 clearly demonstrate the twist effect on breaking strength and indicate that there is an optimum twist level. This phenomenon has been observed in both continuous filament yarns [11] and staple fiber yarns [8]. The initial increase in staple yarn strength with twist is attributed to reduced fiber slippage, while the fall off of strength beyond the optimum twist is attributed to the effect of fiber obliquity.

Concepts such as multiple breaks of components during yarn stretching, the continuing contribution of a broken component to yarn strength, the important role that lateral pressure plays in determining the apparent strength of each component segment, and the behavior of yarn rupture and the statistical nature of yarn strength have not been satisfactorily incorporated into existing yarn models, although they have been explored in single filament composites [12, 13, 14, 28]. In this article, we introduce a new yarn model based on the experimental evidence and concepts for approaching the problem discussed earlier.

The model presented here is an extension of the Monte Carlo model for predicting woven fabric tensile failure proposed by Boyce *et al.* [3]. Their model consists of an array of stochastic elements, each of which is assigned a strength and exhibits various interactions with its neighbors by means of load sharing rules. The manner in which the strengths are determined from the data and assigned to elements are critical aspects of the model, as are the interaction/load sharing rules. As the model is strained, weaker elements will fail and the load will be redistributed to local neighbors by the load sharing rules. Additional strain is then applied, more elements fail, and so on, until final complete failure of a cross section occurs.

For the blended yarn model proposed here, the yarn is modeled as an array of stochastic elements where the array columns are the individual components (the filaments), and each component is further discretized into segments (forming the rows of the arrays). The properties (strength) and behavior (critical length and load sharing rule) of each segment strongly depend on the component type (cotton or polyester) and the lateral pressure, which, in turn, depends strongly on twist level and yarn extension, both of which provide a strong dependence of lateral pressure on the radial position of a component (filament). This dependence on yarn extension necessitates an evolution in element properties and behavior with yarn straining. Strengths are then assigned to elements using a random number generator through a Weibull distribution function for the component, where the Weibull distribution depends on the component's length. Once initial strengths are assigned to each element, a strain increment is applied to the yarn, the weakest element fails, and the load is locally redistributed. Load sharing depends on local lateral pressures and the proximity of the unbroken element to the broken element. Strain is then increased, the weakest element fails, and the entire updating process is repeated.

Consequently, the whole issue of predicting the failure process and ultimate strength of a blended yarn can be posed as a question of predicting the statistical strength of a twisted structure of component bundles with decreasing length and increasing strengths.

The brief computation process of this model is as follows:

1. Model yarns are constructed containing the same constituent filaments and filament placement as those examined experimentally [20] to enable a direct comparison of experimental and predicted results. The blended model in question consists of the same two kinds of components divided into sub-bundles based on the principle of critical length presented above. At each strain increment, analysis of the overall yarn stress level is computed for convenience at the weakest model cross section (the one with the most broken component segments). This is done because the strength of the yarn is governed by the transverse propagation of component filament breakage, as discussed previously.

2. The strengths of the segments are assigned based on values radomly chosen from a Weibull distribution with parameters (shape and scale) calculated from the experimentally observed parameters and the modeled length.

3. The yarn strain increment is taken as the system input. The component strains are then determined based on their respective radial position in the model yarn. The component load is derived on the basis of the given component load-strain curve. Model yarn tension can then be calculated from all of the individual component tensions and the local lateral pressure.

4. Segment failure is determined by comparing segment strength with its component load. Once a component segment is broken, other surviving members in the same cross section will share its load based on the radial position of each surviving member, the distance between

the surviving member and the broken one, and the level of yarn twist and tension.

5. After each increment of model yarn strain, the lateral pressure, critical length of each component segment, and all relevant yarn geometric parameters are updated.

6. Steps 2 through 4 are repeated until the yarn fails, which occurs when all of the segments in one cross section have failed.

Although our model uses the concept of Phoenix's chain-of-bundle approach [25, 26, 27], its extension is significant as a result of the insight derived from the experiments. First, the lateral compression in the yarn is included as a decisive factor. As in Phoenix's work, the effects of twist and component radial location within the yarn are important parameters in our model. Another difference is that in Phoenix's model, the critical length was kept unchanged, while in our model, critical length is determined by component location, component type, and more significantly local lateral compression, and it decreases continuously even before any component break occurs.

ASSUMPTIONS

Because of the complexity of the blended yarn structure, some assumptions are needed to simplify the case so that the model will be mathematically tractable. Note that we are dealing with a model yarn of continuous components, where yarn structural irregularities and the variation of yarn packing density can be considered negligible. The following are our major assumptions:

1. The blended model consists of two kinds of components, first a traditional continuous polyester filament yarn, and second a pseudo-continuous yarn (actually a conventional cotton yarn), each configured in an idealized helix.

2. The number of components in the model yarn cross section is very large (this facilitates the derivation of lateral pressure for the continuum case).

3. The components comprising the model are perfectly flexible so that the torsional and bending stresses within the fibers may be neglected.

4. All components of the same type have identical load versus strain curves, that is, the shape variation of the component load versus strain curves is ignored.

5. The relationship of size (length) and strength of components follows the Weibull distribution.

6. The components are assumed to deform but without change of volume, that is, a component's Poisson ratio is taken to be $\nu_f = 0.5$.

7. This analysis ignores the dynamic effect during the load sharing process after a component is broken.

8. Component breakage will not change the value and distribution of lateral pressure. In other words, Hearle *et al.*'s [11] equations for lateral pressure will be used as described below.

9. To further simplify the problem, we use the average values of such component parameters as initial diameter, specific volume, and the frictional coefficient between components.

As to the yarn parameters and yarn geometry used in the model, we have adopted the relations and equations provided by Hearle *et al.* [11] shown in the following sections. Note that although the results below are derived based on a filament yarn, we assume that they are valid in our model yarn case as well.

YARN PARAMETERS

Yarn helical period (cm), $h = 1/$(turns of twist per cm). Yarn surface helical angle (degrees) is given by

$$\tan \alpha = 0.0112 \phi_y^{1/2} TM \quad , \tag{3}$$

where TM is the yarn twist multiplier. Yarn lateral contraction or Poisson's ratio,

$$\nu_y = -\frac{dR_y/R_y}{dh/h} = -\frac{dR_y/R_y}{\epsilon_y} \quad , \tag{4}$$

where ϵ_y is yarn strain.

GEOMETRY IN A YARN CROSS SECTION

Base angle between adjacent components in nth layer is given by dividing 360° by the number of fibers in each layer n. The radius of the nth layer r_n is

$$r_0 = 0 \tag{5}$$

$$r_{n=1,2,\ldots} = r_{n-1} + r_{c,n-1} + r_{c,n} \quad , \tag{6}$$

where $r_{c,n}$ is the average radius of the components in layer n. The helical angle q for the components in the nth layer is

$$\tan q = \frac{2\pi r_n}{h} \quad . \tag{7}$$

YARN STRAIN VERSUS COMPONENT STRAIN

Because we employ an iterative algorithm in this model, where each iteration can be considered a deformation of infinitesimal strain, we have adopted the result from Hearle *et al.* [11] in an incremental form to govern the yarn and constituent component strain relation:

$$\Delta \epsilon_c = \Delta \epsilon_y (\cos^2 q - \nu_y \sin^2 q) \quad , \tag{8}$$

where ν_y is the Poisson's ratio of yarn, and ϵ_c and ϵ_y are the component strain and yarn strain, respectively.

COMPONENT LOAD VERSUS STRAIN RELATIONSHIP

As we are attempting to simulate the entire yarn fracture process, instead of assuming a Hooke's law between component stress and strain, the pretested component load-strain curves (as in Figure 8) are stored into our algorithm to obtain the load level corresponding to each incremental component strain. Note that the load-strain curves for the cotton and Dacron1 components were actually taken from Monego [20], and we will compare the yarns simulated with these components to those experimentally tested by Monego. The Dacron2 component is artificially designed such that it has an ultimate strength and breaking strain identical to Dacron1 but a different shape, one being convex and the other concave. The comparison of two yarns with the same cotton/polyester blend ratio but made with Dacron1 and 2, respectively, will show how the shape of the component load-strain curve can influence yarn properties.

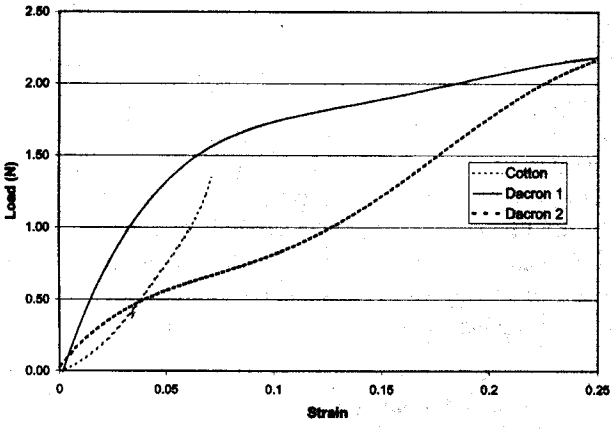

FIGURE 8. Load-extension curves of the components used in the model: (a) the cotton and Dacron1 components [20], (b) the Dacron1 and Dacron2 components.

LATERAL PRESSURE IN A BLENDED YARN

Although there are a few derivations for the distribution of lateral pressure within a yarn, Hearle *et al.*'s result [11] is the most familiar and is assumed to be applicable to our model yarn. We use it here with some minor modifications to suit the blended yarn case.

Even in a blended yarn with different constituent components, the lateral pressure σ_l acting on the different components at the same radial position should be identical because the lateral action and reaction between the components in the same radial positions have to be the same regardless of the component types. According to Hearle's derivations for a monocomponent filament yarn, we have in our case the relation between axial stress σ_y and lateral pressure σ_l:

$$\sigma_y = E_c\epsilon_y\left[\frac{c^2}{u^2} - \nu_y\left(1 - \frac{c^2}{u^2}\right)\right] - 2\nu_c\sigma_l \quad , \qquad (9)$$

where E_c and ν_c are the component modulus and Poisson's ratio, and ϵ_y and ν_y are the model yarn strain and the model yarn Poisson's ratio, whereas

$$u^2 = (1 - c^2)\left(\frac{r_n}{R_y}\right)^2 + c^2 \qquad (10)$$

and

$$c^2 = \cos^2\alpha \qquad (11)$$

are the parameters for component radial positions in the yarn.

Since in our blended yarn there are two different components (components 1 and 2 with blend ratio $b_1 + b_2 = 1$), we have used two forms of Equation 9. For an area of unit area size, with $\nu_{c1} = \nu_{c2} = 0.5$ as assumed before, we obtain

$$\sigma_y = \bar{E}_c\epsilon_y\left[\frac{c^2}{u^2} - \nu_y\left(1 - \frac{c^2}{u^2}\right)\right] - \sigma_l \quad , \qquad (12)$$

where

$$\bar{E}_c = b_1E_{c1} + b_2E_{c2} \quad . \qquad (13)$$

This indicates that the distribution of the lateral pressure within a blended yarn has a form identical to that of a monocomponent yarn as long as a mean modulus $\bar{E}_c$ is used as well as $\nu_{c1} = \nu_{c2}$.

Following the same analysis as Hearle's, the lateral pressure σ_l at radial position r_n in the yarn is

$$\sigma_l = g\bar{E}_c\epsilon_y \quad . \qquad (14)$$

As the "hydrostatic" lateral specific pressure (g/cm^2), σ_l acts perpendicularly to the component axis, and the normalized lateral pressure g at radial position r_n can be expressed as [11]

$$g = \frac{\sigma_l}{\bar{E}_c\epsilon_y} = \frac{c^2}{2}(1 + \nu_y)\left(\frac{1}{u^2} - 1\right) + \nu_y \ln u \quad . \qquad (15)$$

These equations are used in our computer algorithm to calculate and update the distribution of the lateral pressure within the blended yarn.

FILAMENT CRITICAL LENGTH l_c

Theoretically, the effects of yarn structure and extension will affect component mechanical behavior in two ways. One is due to the fact that components within the yarn are under both axial tension and lateral compression. This will lead, as expected, to a mechanical behavior different from a uniaxial case. The second effect is associated with the fragmentation phenomenon. Under the constraint of lateral compression, a component behaves as a chain of mechanically independent segments. Each possesses mechanical properties different from those of other components and other segments in the same component due to the statistical nature of component properties. In our model, only the second factor is included, and we ignore the effect of biaxial loading on component response due to the lack of information about the biaxial properties of the components.

As revealed in the preceding experimental results, a large number of isolated yarn component breaks occur prior to complete model yarn failure. Isolated breaks were also predicted in the fabric tensile strength simulations of Boyce *et al.* [3]. This is similar to what was called the cumulative weakening phenomenon in the fracture of fibrous composite materials that were modeled as being subjected to equal load sharing [5]. As long as the model structure does not collapse, the component breaks will continue to occur until the length of the component segments reaches a minimum value where its load can no longer build up to its segment breaking strength. This length is well known as the critical length. If T_b is the tension that causes the component to break, it follows that the minimum length on which a broken segment can no longer build up its tension again from the broken position or the minimum length into which a component can be broken is [19]

$$l_c = \frac{2T_b}{\pi d \mu \sigma_l} \quad , \tag{16}$$

where μ is the frictional coefficient, d is the component diameter, and σ_l is the local lateral pressure. Note that we will have changing critical lengths at a yarn cross section corresponding to two component types with different T_b and changing lateral pressure at different radial positions.

Remember that this so-called critical length l_c is different from the effective length in relation to fiber slippage in the staple yarn case where fibers tend to slip over each other at their ends due to inadequate frictional gripping. The definition of the effective length in staple yarn [11] is

$$l_e = \frac{T_f}{\pi d \mu \sigma_l} \quad . \tag{17}$$

Since the lateral compression σ_l is approximately proportional to the fiber tension T_f [11], l_e stays largely constant for a given fiber during staple yarn extension. However, l_c decreases as σ_l increases during yarn extension. Although the strength T_b also increases due to segmental shortening, its increase is much less than that of σ_l, so there is no proportionality between T_b and σ_l. In fact, l_c is the maximum value of l_e because T_b is the limit of fiber tension T_f.

FILAMENT STRENGTH VERSUS ITS LENGTH

According to the weakest-link theory [24], statistically the strength of a component will change if its length is altered, following the Weibull distribution [36]. That is, the strength of a component T at any given length l will be

$$F_l(T) = 1 - \exp\left[-\left(\frac{T}{T_l}\right)^p\right] \quad , \tag{18}$$

where T_l is given by

$$T_l = T_0\left(\frac{l}{l_0}\right)^{-1/p} \quad , \tag{19}$$

where T_0 is called the scale parameter and p is the shape parameter.

We tested the strengths of both cotton and Dacron components at a gauge length of $l_0 = 20.32$ cm [20], and the statistical test on the validity of the Weibull distribution involved the Kolmogorov-Smirnov goodness-of-fit test [1] at a significance level of $\alpha > 0.05$. The results fit the two-parameter Weibull distribution quite well. The maximum likelihood estimates of the Weibull shape and scale parameters and the average strengths for both components are summarized in Table I.

TABLE I. Parameters related to component strength.

Parameter	Value	Unit
Gauge length for component strength test	20.32	cm
Average strength of cotton component (based on 20 specimens [20])	1.201	N
Average strength of Dacron component (based on 20 specimens [20])	2.405	N
Weibull shape parameter for cotton component	8.75	
Weibull scale parameter for cotton component	1.513	N
Weibull shape parameter for Dacron component	44.46	
Weibull scale parameter for Dacron component	3.273	N

LOAD SHARING RULE

Although there have been some reports on the mechanism of the load sharing process between broken members and still surviving members during yarn extension

[27, 29], this is still an issue that is poorly understood. Consequently, we will propose a different approach. Note that there is important evidence shown by the experimental results that however the load is shared, it has to be shared locally along the model yarn length, that is, among all surviving component segments at the same yarn cross section where the break took place.

In addition, there is another parameter to be considered—the effect of yarn twist level on the load sharing process. The question is, if a component segment with tension T_b breaks, what is the magnitude of the total extra load shared by all other N_s surviving members? The preceding experimental results show the significant effect of yarn twist level on the yarn strength and fracture behavior, which would lead to a conclusion that for the structures with different twist levels, the load shared from a broken member of strength T_b by all the remaining members should not only depend on T_b, but also on the twist level. In other words, twist will intensify the magnitude of the shared load, similar to the stress concentration effect.

Grosberg and Smith [8] showed that the lateral pressure distribution in a low-twist sliver under extension is proportional to the square of the twist. Here, we have used a load sharing rule that assumes stress concentration due to a broken segment is proportional to the twist multiple. Since it is very difficult to find a feasible means to quantitatively determine the twist effect in the yarn, we have selected a factor for one of the yarns based on our trials on the computer, and we have used that value to model all the other yarns. With this method, the magnitude of the total extra load is $5 \times (TM)^2 T_b$. Furthermore, this load should be shared by all surviving members in the same yarn cross section, and the load shared by one member should be inversely proportional to the distance between this member and the broken one, and should also be related to the ring location of this member in the yarn:

$$\Delta T_{ci} = C \frac{\cos q_i}{r_{bi}} \quad , \tag{20}$$

where ΔT_{ci} is the load shared by member i, r_{bi} is the distance between the two components, and C is a load sharing factor obtained by satisfying

$$\sum_{i=1}^{N_s} \Delta T_{ci} = 5 \times (TM)^2 T_b \quad . \tag{21}$$

YARN-COMPONENT TENSION RELATIONSHIP

Equilibrium provides that the tension on a yarn equals the tension across any yarn section or, in the case of a calculation using a discrete model, to the sum of the tension of all the component segments in any yarn cross section. Hearle *et al.* [11] and others [16, 37] completed the derivations of yarn tension based on the axial stress and lateral compression within the yarn using the continuum approach. However, in the case of a discrete model, the conventional way of calculating yarn tension T_y based on all component tensions is one of summing all component axial tensions T_{ci} discounted by cos q_i, where q_i is the helix angle of the component [27], *i.e.*,

$$T_y = \sum_{i=1}^{N_s} T_{ci} \cos q_i \quad . \tag{22}$$

This method, however, excludes the contribution of lateral pressure to model yarn tension. To illustrate the question, a force equilibrium analysis is desirable. If we take a cut perpendicular to the yarn axis and take a single component segment out of the bundle, we obtain a force equilibrium on this segment, where T_{ci} is the axial component tension in the direction of a helix angle q_i to the yarn axis, and σ_{li} is the circumferencially distributed lateral compression perpendicular to the component axis. A simple force resolution gives the resultant force T_y in the direction of the yarn axis,

$$T_y = \sum_{i=1}^{N_s} \left(T_{ci} \cos q_i - \frac{2}{\pi} \sigma_{li} A_{ci} \sin q_i \tan q_i \right) \quad , \tag{23}$$

where A_{ci} is the cross-sectional area of the component i.

For components parallel to the yarn model axis, so that $q_i = 0$, like those in the yarn center, their contribution to yarn tension will only come from the axial tension T_{ci}, since the lateral compression is balanced or cancelled. However, for other components with $q_i > 0$, the transverse compression contributes to yarn tension.

PARAMETERS UPDATED AFTER EACH ITERATION

The system input of this model is the yarn strain increment $\Delta\epsilon_y$, and all the new parameters after the ith iteration can be obtained using the following equations:

1. Period of helical geometry,

$$h_{i+1} = h_i(1 + \Delta\epsilon_y) \quad , \tag{24}$$

and new yarn length,

$$L_{yi+1} = L_{yi}(1 + \Delta\epsilon_y) \quad . \tag{25}$$

The new length of each component can be similarly updated.

2. Radius of component in layer n,

$$r_{c,n,(i+1)} = r_{c,n,i}(1 - \nu_f \Delta\epsilon_c) \quad , \tag{26}$$

where the component is considered constant volume, that is, $\nu_f = 0.5$.

3. Yarn radius,

$$R_{y,i+1} = r_5 + r_{c,5} \quad , \tag{27}$$

where r_5, the radius of layer 5, is given by Equation 6, and the component radius in layer 5, $r_{c,5}$, is calculated by Equation 26.

4. Yarn lateral contraction,

$$\nu_{yi+1} = \frac{\dfrac{R_{yi} - R_{yi+1}}{R_{yi}}}{\Delta\epsilon_y} \quad . \tag{28}$$

5. Component position, helical angle,

$$\tan q_{n,i+1} = \frac{2\pi r_{i+1}}{h_{i+1}} \quad . \tag{29}$$

Predicted Results and Discussion

Tables I and II summarize all the parameters used in the model. We have simulated a series of cases using the blended yarn model implemented in C++ on a personal computer. Several results predicted by this model are shown below in comparison with the experimental results illustrated previously.

Figures 2, 4, and 5 present both the experimental and theoretical predictions simulating the blended yarns. There is a good agreement between the experimental and predicted load-strain responses. Although the predicted strength and strain at failure is slightly lower for the model results, the general shape and the trends of the experimental data are well captured.

The simulated failure patterns of the components shown in Figures 9, 10, and 11 are at strain levels slightly different from those in the experimental cases. We expected this since the modeled strain at failure was also slightly lower than the experimental response. There is good agreement in the patterns for the yarns of Figures 1 and 9 and Figures 3 and 10. The most visible discrepancy between the experimental and predicted results, however, lies in the pattern of multiple breaks for the blended yarn with 39 cotton components and 52 polyester components. The predicted pattern shows a less concentrated propagation of yarn breaks.

TABLE II. Other component properties used in the model.

Property	Value	Unit
Specific volume of cotton component	0.649	$\frac{cm^3}{g}$
Diameter of cotton component	82.4×10^{-4}	cm
Surface frictional coefficient of cotton component	0.20	
Specific volume of Dacron component	0.725	$\frac{cm^3}{g}$
Diameter of Dacron component	83.7×10^{-4}	cm
Surface frictional coefficient of Dacron component	0.26	

The predicted twist effect on yarn strength and fracture behavior is shown in Figure 12. The load versus strain responses in Figure 12 corresponding to various twist levels are quite close to the experimental ones in Figure 7 for the same yarn model. Both results show a decrease in the slope of the load versus strain curve with an increase in the twist multiple. The trends of twist influence on yarn breaking strength and breaking strain are well captured by the model, but the magnitude of the difference between the values at the various twist levels

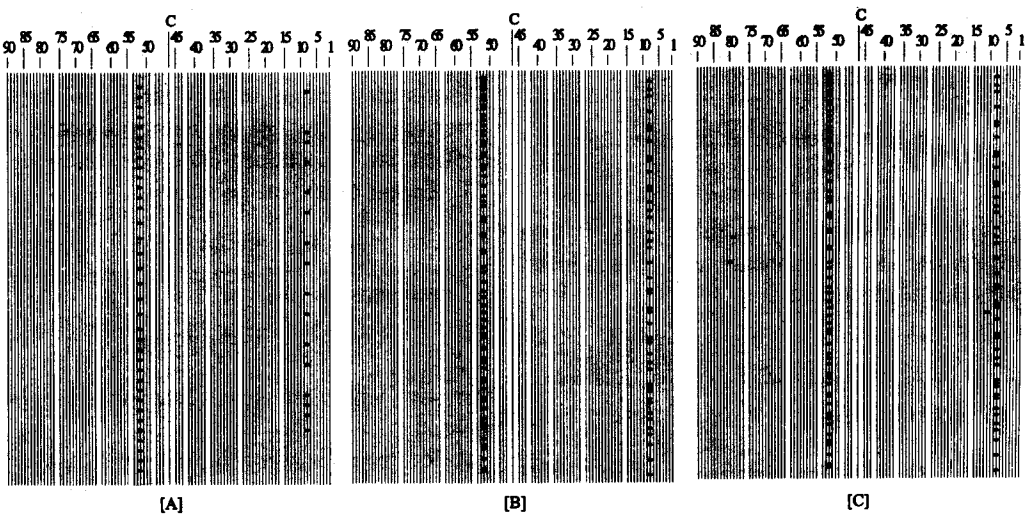

FIGURE 9. Predictions of the model with 2 cotton and 89 Dacron components at TM = 2.19: (a) multiple breaks at 8% extension, (b) multiple breaks at 8.6% extension, (c) multiple breaks at 24% extension.

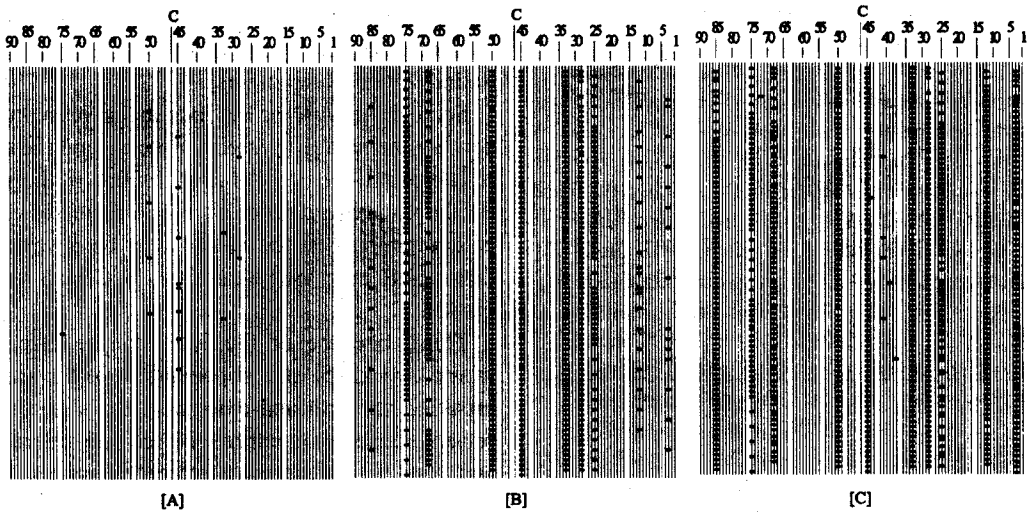

FIGURE 10. Predictions of the model with 11 cotton and 80 Dacron components at $TM = 4.37$: (a) multiple breaks at 7.8% extension, (b) multiple breaks at 9.1% extension, (c) multiple breaks at 19.2% extension.

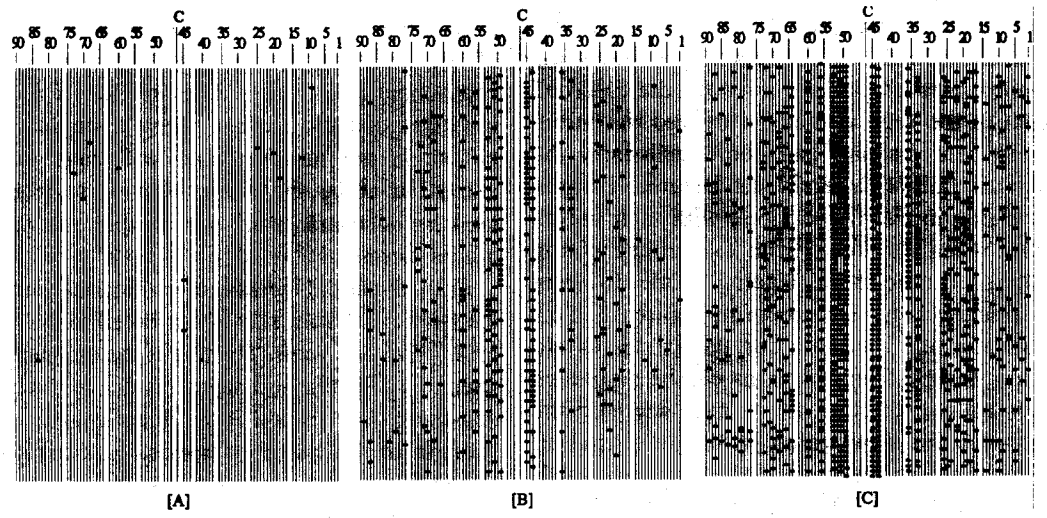

FIGURE 11. Predictions of the model with 40 cotton and 51 Dacron components at $TM = 3.26$: (a) multiple breaks at 7.3% extension, (b) multiple breaks at 8.0% extension, (c) multiple breaks at 8.6% extension.

is not as great as those experimentally observed. For example, the predicted maximum difference in strain to failure (strain at the maximum load) for the set of yarns shown in Figure 12 is 1%, while the observed maximum difference was 5% from Figure 7.

Figure 13 shows the predicted results of two blended yarn models with the same constituent components and identical characteristics, except that the shapes of the stress-strain curves of the Dacron components are different, as shown in Figure 8. The first model used Dacron1, which has a more or less convex shape, while the second used the Dacron2 concave curve. A given strain level generates lower stress in Dacron2 than in Dacron1, as can be easily seen from

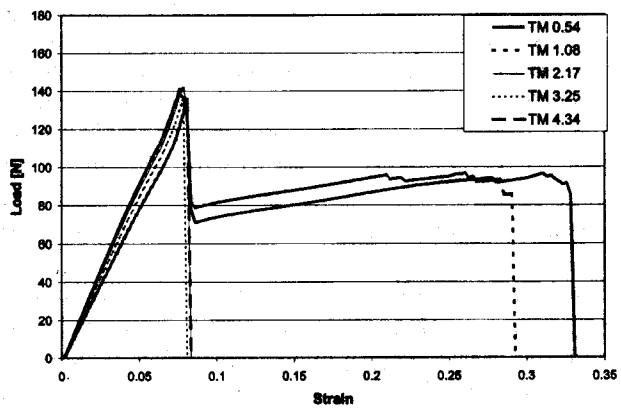

FIGURE 12. Effects of twist level on the fracture behavior of yarn models (predicted).

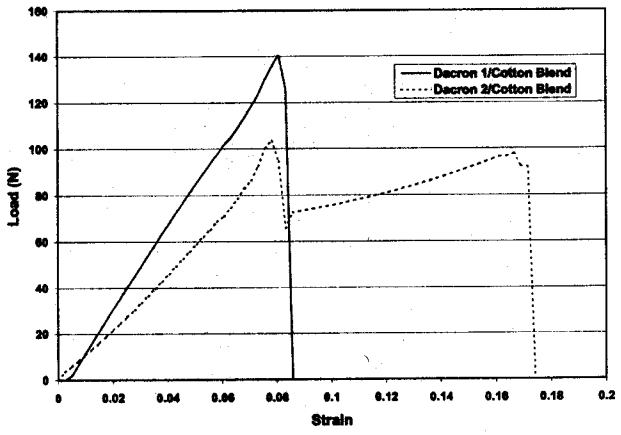

FIGURE 13. Predicted shape effect of component load-extension curves.

their load-strain curves. In other words, at the same strain level, Dacron2 components will have more potential to share a load without failure than Dacron1, when a component breaks. As a result, the Dacron2 components in the second model survived the initial cotton component fracture and could still carry the load until final failure, whereas the Dacron1 components in the first model failed along with their cotton counterparts when the loads from the broken cotton components shed onto them, leading to the different system of fracture behavior shown in Figure 13. This clearly indicates the potential for the model to aid blended yarn design. Blended yarns can be simulated before they are constructed, which may decrease the time to market for new yarns. Also, this kind of modeling can lead to the design of fibers with load-strain responses that will be used to construct yarns with the mechanical responses desired.

Conclusions

This study has involved a real synthetic filament yarn and a pseudo-filament yarn (staple cotton) whose load-elongation properties are drastically different. When combined in a blended structure, the pseudo-filament system is subjected to early failure of the more brittle component, leading to fragmentation and overall structural softening, and even stepwise load reduction.

Although the predicted results we present are limited and there are still many more cases to be investigated with this model, we can draw a few conclusions. First, contrary to Hearle *et al.*'s well accepted conclusion that "In continuous-filament yarns, twist is not necessary for the attainment of tensile strength (in fact, it reduces it) [11].", our study shows that twist-caused lateral pressure considerably raises the overall strength of a blended yarn by increasing the apparent strengths of the segments of its individual components.

Second, because of the increasing strength of component segments due to lateral pressure and the dependence of lateral pressure on the ring location in the yarn model, for the same blend ratio, the ring location of certain kinds of components in the model will be a very significant factor and may lead to entirely different yarn fracture results.

Third, because of the load sharing effect, in cases where two kinds of components have the same average breaking strength and extension, the shape of the component stress-strain curve will become a dominant factor and may have a decisive effect on system fracture behavior.

Fourth, yarn tension should be equal to the tension of any cross section of the yarn. However, as there are different numbers of active (load carrying) component segments on each cross section after the initial breaks of the constituent components, the tension on each component at different cross sections may vary. This indicates that the tension along a single whole component is not uniform, and will cause an irregular extension along the component as supported by the necking mechanism of the components in a broken model sample.

Fifth, the initial increase of continuous yarn tenacity as the twist rises from zero is attributed to the lateral compression in two ways. The first is the increasing apparent strength of the filament segments due to the rising lateral constraint. The second is the direct contribution to yarn strength of the lateral compression acting on those inclined components, which becomes more significant as the twist increases.

Sixth, another important issue revealed in this study is the influence of a structure on its constituent components during loading. A similar mechanism has been reported in fabric studies [3, 18, 34] where the interactions of those components (yarns) during fabric extension will enhance the apparent strength of the yarns so that the overall strength of the fabric will be much higher than that calculated based on individual isolated yarns. This structural assistance mechanism should be used in reinforcing some fibrous structures.

Finally, because of this structural assistance, it is often meaningless to deal with the mechanical properties of the constituent components isolated from a specific structure, since these properties will alter once the component is assembled into the structure. It may be desirable to designate new conditions (close to the real situation of the structure) under which the properties of the component should be determined.

ACKNOWLEDGMENTS

We would like to thank the Fibers Department of E. I. du Pont de Nemours & Co. for providing financial and technical support for this work, and for the guidance and encouragement of staff member Dr. Don Shiffler (currently at North Carolina State University). We acknowledge Warren Taylor, who translated the program from FORTRAN to C++ and improved the efficiency of the algorithm. This study is part of a broad program at MIT and Georgia Institute of Technology on the translation of fiber properties into yarn and fabric behavior.

Literature Cited

1. Breiman, L., "Statistics: With a View Toward Applications," Houghton Mifflin Company, Boston, MA, 1973.
2. Backer, S., Staple Fibers: The Story of Blends, in "Polyester: 50 Years of Achievement," D. Brunnschweiler and J. W. S. Hearle, Eds., Textile Institute, U.K., 1993, p. 94.
3. Boyce, M. C., Palmer (Realff), M. L., Seo, M., Schwartz, P., and Backer, S., A Model of the Tensile Failure Process in Woven Fabrics, *J. Appl. Polym. Sci. Appl. Polym. Symp.* **47,** 383 (1991).
4. Dogu, I., The Distribution of Transverse Pressure in a Twisted Yarn Allowing for the Fiber Migration and Variation of Fiber Packing Density, *Textile Res. J.* **42,** 726 (1972).
5. Dow, N. F., Study of Stress Near a Discontinuity in a Fiber-Reinforced Composite Metal, Space Mechanics Memo no. 102, GE Space Sciences Lab, Jan. 1961.
6. Galileo, Galilei, "Dialogue Concerning Two New Sciences," Leyden (1638), translated by A. De Salvio and A. Fabaro, Evanston, IL, 1914.
7. Gottfried and Byron, S., "Elements of Stochastic Process Simulation," Prentice-Hall, NY, 1984.
8. Grosberg, P., and Smith, P. A., The Strength of Slivers of Relatively Low Twist, *J. Textile Inst.* **57,** 15 (1966).
9. Gurney, H. P., Distribution of Stress in Cotton Products, *J. Textile Inst.* **16,** 269 (1925).
10. Hamburger, W. J., The Industry Application of the Stress-Strain Relationship, *J. Textile Inst.* **40,** 700 (1949).
11. Hearle, J. W. S., Grosberg, P., and Backer, S., "Structural Mechanics of Yarns and Fabrics," vol. 1, Wiley-Interscience, NY, 1969, p. 180.
12. Hui, C. Y., Phoenix, S. L., Ibnabdeljalil, M., and Smith, R. L., An Exact Closed Form Solution for Fragmentation of Weibull Fibers in a Single Filament Composite with Application to Fiber Reinforced Ceramics, *J. Mechan. Phys. Solids* **43,** 1551–1585 (1995).
13. Hui, C. Y., Phoenix, S. L., and Kogan, L., Analysis of Fragmentation in the Single Filament Composite: Roles of Fiber Strength Distributions and Exclusion Zone Models, *J. Mechan. Phys. Solids* **44,** 1715–1737 (1996).
14. Hui, C. Y., Phoenix, S. L., and Shia, D., The Single Filament Composite Test: A New Statistical Theory for Estimating the Interfacial Shear Strength and Weibull Parameters for Fiber Strength, *Composites Sci. Technol.* **57,** 1707–1725 (1998).
15. Kemp, A., and Owen, J. D., The Strength and Behavior of Nylon/Cotton Blended Yarns Undergoing Strain, *J. Textile Inst.* **46,** T-684 (1955).
16. Kilby, W. F., The Mechanical Properties of Twisted Continuous-Filament Yarns, *J. Textile Inst.* **55,** T589 (1964).
17. Lord, P. R., Yarn Modeling—A Discussion of the Needs and Opportunities, in "Proc. Cotton Incorporated Miniconference," Nov. 3–4, 1988.
18. Lord, P. R., and Radhakrishnaiah, P., A Comparison of Various Woven Fabrics Containing Friction, Rotor, and Ring Spun Cotton Yarn Fillings, *Textile Res. J.* **58,** 354 (1988).
19. Machida, K., Mechanics of Rupture in Blended Yarns, Masters thesis, M.I.T., Cambridge, MA, 1963.
20. Monego, C. J., The Mechanics of Rupture of Cotton-Dacron Yarns, Masters thesis, M.I.T., Cambridge, MA, 1966.
21. Monego, C. J., and Backer, S., Tensile Rupture of Blended Yarns, *Textile Res. J.* **38,** 762 (1968).
22. Monego, C. J., Backer, S., Qui, Y. P., and Machida, K., Illustration of Stress-Strain Behavior and Yarn Fragmentation in a Pseudo-Hybrid Composite System, *Composite Sci. Technol.* **50,** 451 (1994).
23. Noshi, H., Shimadu, M., and Kusano, T., Study on Blended Yarns, Part I: The Tensile Strength of Twisted Yarn Consisting of Two Kinds of Continuous Filaments, *J. Textile Mech. Soc.* **42,** 91 (1959).
24. Peirce, F. T., Tensile Tests for Cotton Yarns, V: 'The Weakest Link'—Theorems on the Strength of Long and of Composite Specimens, *J. Textile Inst.* **17,** 355 (1926).
25. Phoenix, S. L., Probabilistic Strength Analysis of Fiber Bundle Structures, *Fiber Sci. Technol.* **7,** 15 (1974).
26. Phoenix, S. L., Probabilistic Inter-fiber Dependence and the Asymptotic Strength Distribution of Classic Fiber Bundles, *Int. J. Eng. Sci.* **13,** 287 (1975).
27. Phoenix, S. L., Statistical Theory for the Strength of Twisted Fiber Bundles with Applications to Yarns and Cables, *Textile Res. J.* **49,** 407 (1979).
28. Phoenix, S. L., Ibnabdeljalil, M., and Hui, C. Y., Size Effects in the Distribution for Strength of Brittle Matrix Fibrous Composites, *Inst. J. Solids Struct.* **34,** 545–568 (1996).
29. Pitt, R. E., and Phoenix, S. L., On Modeling the Statistical Strength of Yarns and Cables Under Localized Load-Sharing Among Fibers, *Textile Res. J.* **51,** 408 (1981).
30. Platt, M. M., Mechanics of Elastic Performance of Textile Materials, Part III: Some Aspects of Stress Analysis of Textile Structures—Continuous Filament Yarns, *Textile Res. J.* **20,** 1 (1950).
31. Ratman, T. V., *et al,* Prediction of the Quality of Blended Yarns from That of the Individual Components, *Textile Res. J.* **38,** 360 (1968).
32. Realff, M. L., Seo, M., Boyce, M. C., Schwartz, P., and Backer, S., Mechanical Properties of Fabrics Woven from Yarns Produced by Different Spinning Technologies: Yarn

Failure as a Function of Gauge Length, *Textile Res. J.* **61**, 517–530 (1991).
33. Rosen, B. M., "Fiber Composite Materials," American Society for Metals, OH, 1965, p. 37.
34. Shahpurwala, A. A., and Schwartz, P., Modeling Woven Fabric Tensile Strength Using Statistical Bundle Theory, *Textile Res. J.* **59**, 26 (1989).
35. Sullivan, R. R., A Theoretical Approach to the Problem of Yarn Strength, *J. App. Phys.* **13**, 157 (1942).
36. Weibull, W., A Statistical Distribution Function of Wide Application, *J. Appl. Mech.* **18**, 293 (1951).
37. White, J. L., Chen, C. C., and Spruiell, J. E., Some Aspects of the Mechanics of Continuous Filament Twisted Yarns and the Deformation of Fibers, *App. Polym. Symp.* (27), 275 (1975).

Manuscript received November 6, 1998; accepted April 27, 1999.